Journal of Colloid and Interface Science 633 (2023) 786–799

Contents lists available at ScienceDirect

Journal of Colloid and Interface Science

journal homepage: www.elsevier.com/locate/jcis

Elucidating the mechanisms of action of antibiotic-like ionic gold and biogenic gold nanoparticles against bacteria

Monica Paesa [a,b], Cristina Remirez de Ganuza [a,b], Teresa Alejo [a,b,c,d], Cristina Yus [a], Silvia Irusta [a,b,c,d], Manuel Arruebo [a,b,c,d,*], Víctor Sebastian [a,b,c,d,*], Gracia Mendoza [c,d]

[a] Department of Chemical Engineering, University of Zaragoza, Campus Río Ebro-Edificio I+D, C/ Poeta Mariano Esquillor S/N, 50018 Zaragoza, Spain
[b] Instituto de Nanociencia y Materiales de Aragón (INMA), CSIC-Universidad de Zaragoza, Zaragoza 50009, Spain
[c] Aragon Health Research Institute (IIS Aragon), 50009-Zaragoza, Spain
[d] Networking Research Center on Bioengineering, Biomaterials and Nanomedicine, CIBER-BBN, 28029-Madrid, Spain

GRAPHICAL ABSTRACT

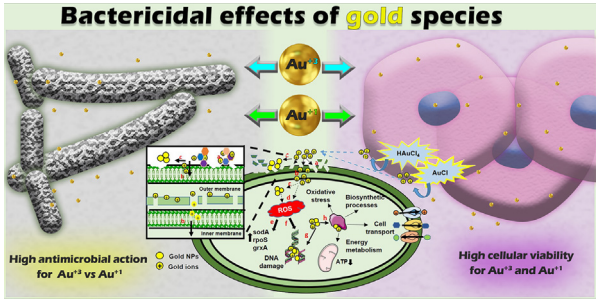

ARTICLE INFO

Article history:
Received 22 August 2022
Revised 17 November 2022
Accepted 27 November 2022
Available online 28 November 2022

Keywords:
Ionic gold
Gold nanoparticles
Antimicrobials
Pathogenic bacteria
Cellular damage
Oxidative stress
Proteomics
Genomics

ABSTRACT

The antimicrobial action of gold depends on different factors including its oxidation state in the intra- and extracellular medium, the redox potential, its ability to produce reactive oxygen species (ROS), the medium components, the properties of the targeted bacteria wall, its penetration in the bacterial cytosol, the cell membrane potential, and its interaction with intracellular components. We demonstrate that different gold species are able to induce bacterial wall damage as a result of their electrostatic interaction with the cell membrane, the promotion of ROS generation, and the consequent DNA damage. In-depth genomic and proteomic studies on *Escherichia coli* confirmed the superior toxicity of Au (III) vs Au (I) based on the different molecular mechanisms analyzed including oxidative stress, bacterial energetic metabolism, biosynthetic processes, and cell transport. At equivalent bactericidal doses of Au (III) and Au (I) eukaryotic cells were not as affected as bacteria did, maintaining unaffected cell viability, morphology, and focal adhesions; however, increased ROS generation and disruption in the mitochondrial membrane potential were also observed. Herein, we shed light on the antimicrobial mechanisms of ionic and biogenic gold nanoparticles against bacteria. Under selected conditions antibiotic-like ionic gold can exert a strong antimicrobial activity while being harmless to human cells.

* Corresponding authors at: Department of Chemical Engineering, University of Zaragoza, Campus Río Ebro-Edificio I+D, C/ Poeta Mariano Esquillor S/N, 50018 Zaragoza, Spain.
E-mail addresses: arruebom@unizar.es (M. Arruebo), victorse@unizar.es (V. Sebastian).

https://doi.org/10.1016/j.jcis.2022.11.138
0021-9797/

1. Introduction

Antibiotic resistant bacteria constitute a global threat for human, animal and environmental health, development, and sustainability. Considering that there is a direct association between antibiotic use and antibiotic resistance, and despite all the efforts and awareness campaigns on antimicrobial resistance (AMR), more than 2.8 million AMR-associated infections occur in the US per year according to a 2019 report, causing more than 35,000 fatalities [1]. In the EU, 33,110 deceases were attributed in 2015 to AMR and healthcare-associated infections account for 75% of the burden of disease [2]. Basic, translational and clinical research projects are focused on different areas aiming to tackle the problem including the development of novel antimicrobials. One of the requirements for a novel antibacterial compound is its demonstrated lack of known cross resistance. Metal-based compounds including organometallic compounds, ionic solutions, complexes and colloidal dispersions were formerly used to treat pathogenic bacteria but they were displaced with the discovery of antibiotics because of the selectivity towards prokaryotic cells of the latter. However, most of the antibiotics have a single molecular target on bacteria and therefore the chances to develop genetic mutations, and therefore resistance, are higher than those present in metal-based compounds where multiple mechanism of antimicrobial action take place simultaneously. Those reported mechanisms include the production of ROS, the inactivation of antioxidants; protein dysfunction and loss of enzymatic activity; damage to cellular membranes, disruption of electron transport and prevention of ATPase activity; interference with nutrient acquisition; genotoxicity; irreversible binding to donor ligands (including extra- and intracellular proteins and enzymes), among others [3].

Compared to other heavy metals, elemental bulk gold shows reduced cytotoxicity against eukaryotic cells due to its limited solubility and low reactiveness and due to its high electronegativity and standard reduction potential which prevent it from oxidation. In general, the toxicity to microorganisms of common metals increases following the sequence: Ag > Hg > Cu > Cd > Cr > Pb > Co > Au [4]. However, as gold particle size decreases, solubility increases and ionic gold can be released producing cytotoxic and genotoxic effects derived from the combined effects of both reduced particle size (e.g., membrane damage) and particle dissolution mainly due to the ability of ionic gold to bind DNA and interrupt transcription [5]. It has been demonstrated that after intravenous administration, gold nanoparticles biodegradation in preclinical models is slow, e.g., only $\approx$ 4% of the administered dose is excreted from the liver and the kidneys within one month when using pegylated hollow gold nanoparticles [6] and their repeated administration causes bioaccumulation mainly in organs of the mononuclear phagocytic system, significantly in the liver [7].

In addition, in eukaryotic cells, the reductive intracellular environment can change the oxidation state of gold precursors and nanoparticles as part of a dynamic process. In this regard, Balfourier et al. [8] demonstrated that gold nanoparticles are rapidly up-taken via endocytosis inside eukaryotic cells where initially are biodegraded due to the dual action of the membrane-bound NADPH oxidase and the acidic environment of the endosomal-lysosomal system and successively, metal-binding proteins (e.g., metallothioneins) biomineralize those dissolved species rendering again recrystallized metal nanoparticles.

The antimicrobial action of gold depends on its speciation state (ionic or zerovalent), its coordinating ligands (e.g., phosphine-type, Au-C bonds in organogolds, etc.) its size, morphology, specific surface area, electrokinetic potential, purification degree and agglomeration state when nanoparticulated, and on its pH, solubility and bioavailability when present as inorganic gold (e.g., aqueous solutions of $AuCl_3$, $HAuCl_4$, etc.) [9,10]. Also, its antimicrobial action depends on the presence or absence of light to induce photodynamic effects [11], the contact between the pathogenic microorganism and the gold-based material [12], and the ligands present on the surface in case of gold-based nanoparticles. In this regard, Cui et al. [13] demonstrated that, by selecting the appropriate surface modification on gold nanoparticles, even ROS generation can be halted and the bactericidal effect just attributed to energy-metabolism arrest, by inhibiting ATP synthase activity and transcription of bacteria inhibition by impeding a subunit of the ribosome from tRNA binding. Therefore, the antimicrobial mechanism of action can be tuned depending on the appropriated nanoparticle surface modification.

Gold nanoparticles are not internalized by bacterial cells due to their lack of endocytic pathways and due to their restricted pass towards their inner cytosols. In this regard, the porosity of the outermost peptidoglycan layer in Gram-positive bacteria and the inner peptidoglycan layer of Gram-negative bacteria show a pore size cut-off of less than 3 nm [14] and the largest reported porin in the outer membrane of *Escherichia coli* (i.e., the SecA subunit of the protein secretion complex) is reported to have less than 6 nm in diameter [15]. Therefore, metallic gold nanoparticles are largely excluded from diffusing to the interior of bacteria unless having cluster sizes or in partially damaged bacteria when membrane disruption occurs. In this regard, Zheng et al. [16] showed that Au clusters having less than 2 nm in size were internalized by *Staphylococcus aureus* whereas Au nanoparticles of larger sizes (>3 nm) and having the same surface ligand (p-mercaptobenzoic acid) and concentration were excluded and, consequently intracellular antimicrobial action was only reported for the former. Ionic gold can easily diffuse to the interior of the bacterial cytosol exerting bacteriostatic (e.g., MBC (minimum bactericidal concentration)/MIC (minimum inhibitory concentration) > 4), or bactericidal (e.g., MBC/MIC $\leq$ 4) effects depending on its dose, or even acting as a source of metallic zerovalent gold during a reductive biomineralization process as part of a natural detoxification course in several bacteria [17]. This biomineralization can take place not only in the reductive interior environment of bacteria but also in the extracellular space as attributed to the reductive character of some of the polysaccharides and proteins secreted by Gram-positive and Gram-negative bacteria in order to antagonize the potential toxicity of ionic gold [18]. Au (I) and Au (III) antibacterial action has been reported on Gram-positive and Gram-negative bacteria being mainly dependent on the exposure time and on the presence of buffers [9,19]. Moreover, compared to different antibiotics, previous studies have demonstrated higher or equal antimicrobial ability for gold species in the eradication of the Gram-negative bacteria *Pseudomonas aeruginosa* [20]. To counteract the antimicrobial action of ionic gold, natural bacterial detoxification is based on exporting those ions to reduce their intracellular accumulation to prevent damage, likely utilizing ATPase metal efflux proteins commonly utilized for a wide range of metals and also by reducing the potentially toxic ionic gold in the extracellular space thanks to the action of their secreted polysaccharides (e.g., hemiacetal groups in *E. coli* and *Bacillus subtilis*). The ionic gold antimicrobial action also depends on the composition of the culture medium and the specific bacteria tested.

In the search for alternatives to antibiotics we have previously studied the effects of chitosan-gold nanocomposites in prokaryotic and eukaryotic cells [12] but also in an *in vitro* coculture model of human macrophages infected with *S. aureus* or *E. coli* [21]. These studies have revealed the efficient antibiotic-like bactericidal effect of gold-based nanocomposites without damaging mammalian cells at equivalent doses. Interestingly, chitosan was not found to exert antibacterial activity at the deacetylation degrees and molecular

weights used. In order to elucidate the role of gold in the bactericidal mechanisms, we have analyzed, in the present work, the cytotoxic action of ionic gold on eukaryotic and prokaryotic cells and selected specific Au (I) and Au (III) concentrations for which the cytotoxicity against eukaryotic cells is largely excluded (analyzing cell cycle, cell metabolism, ROS induction, and membrane damage) while being antimicrobial against *E. coli* S17 strain and *S. aureus* ATCC 25923.

2. Material and methods

Materials and methods and associated references are available in the supplementary Information section.

2.1. Evaluation of Au (III) and Au (I) effects on bacteria

To investigate the mechanisms by which gold precursors eradicate bacteria, five analytical methodologies were performed: Scanning electron microscopy (SEM); Transmission electron microscopy (TEM); Fourier Transform Infrared (FTIR) and UV–VIS spectroscopy; and X-ray photoelectron spectroscopy (XPS).

A scanning electron microscope equipped with an energy X-ray dispersive spectroscopy (EDS) analyzer was carried out to study the changes in the bacterial morphology after gold precursors treatment following our previously reported methodology [21]. After 24 h of treatment, bacterial samples were washed twice in PBS 0.1 M and fixed in 2.5% glutaraldehyde overnight at room temperature. Then, samples were filtered (0.2 μm, pore size cut-off) and subsequently dehydrated in a series of ethanol solutions (30–100%; twice for 15 min). The solvent was evaporated at room temperature to allow a subsequent coating with a thin layer of metal (Pt, 15 nm) to allow electronic observation. SEM images were acquired using a SEM Inspect F50 (FEI Co., USA) operating at an accelerating voltage of 10–15 keV.

To study the gold nanostructures distribution in the microbiological samples, bacteria were treated with Au (III) and Au (I) species and washed twice with PBS 0.1 M. Then, the bacterial pellet was collected, resuspended in ultrapure water and observed by TEM using a FEI Tecnai T20 microscope operating at 200 kV.

To confirm the specific interaction of gold species with the bacterial surface, FTIR spectra of the untreated and Au (III) or Au (I) treated bacteria were recorded on a Bruker Vertex 70 FTIR spectrometer equipped with an ATR Golden Gate accessory and using a DTGS detector. Initially, *E. coli and S. aureus* cells (10^5 CFU/mL) were treated with different concentrations of Au (III) and Au (I) for 24 h. After centrifugation, dried pellets were deposited on a glass cover and spectra were recorded by averaging 40 scans in the 4000–600 cm^{-1} wavenumber range at a resolution of 4 cm^{-1}.

Gold stock solutions (10 mM) and the highest gold species concentration used (125 μM) were incubated with bacteria-free TSB medium for 24 h and gold nanoparticle (AuNP) formation was monitored via UV–VIS spectroscopy recording the characteristic surface plasmon resonance band attributed to AuNPs. Measurements were carried out in a double beam UV–VIS spectrophotometer (PerkinElmer Lambda 35) over a range between 350 and 800 nm.

For XPS measurements, *E. coli* and *S. aureus* cells (10^5 CFU/mL) were treated with different concentrations of Au (III) and Au (I) for 24 h. After centrifugation, bacteria were washed and dried pellets were deposited on a glass coverslip. Bacteria samples were analyzed using AXIS Supra spectrometer (Kratos Analytical Ltd., UK) with a monochromatic Al Kα radiation (hυ=1486.6 eV) as excitation source. XPS spectra were analyzed using the Casa XPS program with the Shirley function background correction and peak fitting was performed using a Gaussian-Lorentzian function. The recorded binding energy (BE) spectra were corrected with reference to aliphatic carbon set at 285 eV.

Taking into account the differential effects obtained in the described methodologies regarding Gram-positive and Gram-negative bacteria and the bactericidal results (see subsequent sections where the lack of antimicrobial action against Gram-positive bacteria is shown), all experiments from these assays were only performed in the Gram-negative bacteria model studied, *E. coli*.

2.2. Au NPs formation and oxidative stress induction

To further elucidate the mechanism of AuNP formation, *E. coli* samples (10^5 CFU/mL) were treated with 125 μM Au (III) or Au (I) for 24 h. Then, bacteria were centrifuged (13,000 rpm, 5 min) and the supernatant was analyzed by UV–VIS to evaluate the potential presence of Au NPs. Afterwards, the supernatant was also centrifuged (13,000 rpm, 30 min), and the pellet was resuspended in ultrapure water and visualized by TEM.

To assess whether bacteria exudates could reduce ionic gold species, *E. coli* samples (10^5 CFU/mL) were centrifuged (13,000 rpm, 5 min). The bacteria-free supernatant was collected, mixed with 125 μM Au (III) or Au (I) and observed again by UV–VIS to identify the presence of the characteristic surface plasmon resonance peak attributed to the presence of Au NPs. Afterwards, the supernatant was centrifuged (13,000 rpm, 30 min) and the resulting pellet was resuspended in ultrapure water and visualized by TEM.

ROS generation was assessed using the oxidation-sensitive probe dihydrorodamine 123 (DHR 123) following the manufacturer's instructions. Briefly, *E. coli* samples were exposed for 15 min to Au (III) (62.5 and 125 μM) or to Au (I) (125 μM). Then, cultures were centrifuged, washed with PBS 0.1 M and incubated for 30 min in the dark with the same buffer containing the probe (40 μM final concentration) at 37 °C. Bacteria were subsequently washed and pellets suspended in 1 mL of the same buffer. Fluorescence intensity (excitation at 488 nm and emission at 530 nm) was monitored by flow cytometry (FACSARIA BD equipment and software, USA).

2.3. Nucleic acid release measurement

To demonstrate whether the bactericidal mechanism of gold is mediated by cell wall disruption, the amount of released nucleic acids was determined from the maximum absorbance at 260 nm using a NanoDrop 2000 spectrophotometer (ThermoFisher Scientific, US). Briefly, *E. coli* was incubated with Au (III) 62.5 μM or Au (I) 125 μM for 2 and 4 h in TSB. The bacterial suspensions were centrifuged (3,500 rpm, 5 min) and the supernatants optical density (OD) was then measured at 260 nm.

2.4. Genetic response to oxidative stress

E. coli samples (10^7 CFU/mL) were incubated with Au (III) 62.5 μM or Au (I) 125 μM for 2 h to evaluate genetic expression by quantitative RT-PCR. Cells were washed with PBS and lysed with RNAeasy mini kit (Qiagen, Germany) following the manufacturer's instructions. RNA was reverse transcribed with High-Capacity cDNA Reverse Transcription Kit (Applied Biosystems, US) and quantified by means of NanoDrop® 8000 (ThermoFisher Scientific, US). The amplification was carried out using Power SYBR Green PCR Master Mix (Applied Biosystems, US) on a 7900HT Fast Real-Time PCR System (Applied Biosystems, US). Genes related to stress responses (*oxyR, rpoS, sodA*) and two thiol-disulphide oxidoreductases (*grxA, trxA*) were selected for the analysis. Gene expression was normalized to the level of the *gapA* gene used as reference. Sequences of the primer pair sets are listed in

Table S1. The values obtained from tested genes were normalized to those obtained in the control groups (non-treated cells). Three independent experiments were performed in triplicate and the results were represented as a mean ± SD.

2.5. Global proteome analysis of E. coli: Sample preparation for LC-MS/MS

E. coli samples (10^7 CFU/mL) were treated with Au (III) 62.5 μM or Au (I) 125 μM for 2 h. Samples were centrifuged and pellets were resuspended in a lysis buffer consisting of NP40 Cell Lysis Buffer (Sigma-Aldrich, US) plus complete ™ Mini Protease Inhibitor Cocktail (Sigma-Aldrich, US) and then mechanical lysis was performed using sonication (SONOPULS HD 2200 ultrasonic homogenizer) (60 W, 20 kHz, 3 cycles per sample: 45 s at 70% power, 2 min dwell time). Cell debris was removed by centrifugation (13,300g, 20 min, 4 °C). Total protein was quantified using the Pierce™ Detergent Compatible Bradford Assay Kit (ThermoFisher Scientific, US). Buffer exchange was performed by using Amicon® Ultra 0.5 mL Filters (Sigma-Aldrich, US) following the manufacturer's instructions. Then, samples were resuspended in denaturing buffer (6 M urea, 100 mM Tris buffer pH 7.8). Next, cysteines were reduced with DTT (200 mM) for 30 min at 37 °C and alkylated with iodoacetamide (200 mM) for 30 min in the dark. Unreacted iodoacetamide was consumed adding 200 mM DTT for 30 min at room temperature. Then, samples were diluted with 50 mM ammonium bicarbonate to a final concentration lower than 1 M of urea. Digestion was carried out overnight with the enzyme trypsin (Gold Trypsin, Promega) at 37 °C and a 1:20 ratio (enzyme/protein). Reaction was stopped by adding concentrated formic acid (Sigma-Aldrich, US).

The digested peptides (1.2 μg) were analyzed by nano-liquid chromatography and concentrated by reverse phase chromatography. Then, samples were separated on an analytical reverse phase C18 Picofrit column with a flow rate of 250 nL/min. The eluents consisted of buffer A (0.1% (v/v) formic acid (FA), H_2O) and buffer B (0.1% (v/v) FA, ACN (Acetonitrile)), and the peptides were eluted using a gradient from 2% to 40% of buffer B over 180 min. The eluted peptides were electro-sprayed directly into the Q Exactive HF mass spectrometer. Survey MS scans ranged from 350 to 2000 Da. MS/MS data were acquired running a data-dependent acquisition (DDA) method. The spectra were acquired in positive mode.

MS/MS spectra were processed using the Proteome Discoverer 2.4 (ThermoFisher Scientific, US) software with MASCOT search engine v.2.6.1. Uniprot databases were used with taxonomic restriction to *E. coli* (UP00000625.fasta) (4348 sequences). The identification was performed according to the following parameters: proteolytic enzyme: trypsin; fixed modification: carbamidomethylation of cysteine; variable modifications: oxidation of methionine and acetylation of the amino terminal; precursor ion mass tolerance of ±10 ppm; fragment ion mass tolerance of 0.02 Da; and two missed cleavages were allowed. For all runs, the false discovery rate (FDR) was set to <0.01 for peptide identification. Proteins with a minimum fold change of 1.5 and $p < 0.05$ (Au(I)/Control (CT) and Au(III)/CT) were considered to regulate differently.

2.6. Gold cytotoxicity evaluation

Fibroblasts and macrophages were seeded onto 96-well plates at 6×10^3 and 7×10^4 cells per well, respectively. The cytotoxicity of different Au (III) and Au (I) concentrations (31.25–250 μM) was evaluated using the Blue Cell Viability Assay (Abnova, Taiwan) after 24 h of incubation. Then, the reagent was added following the manufacturer's indications (10%; 4 h at 37 °C and 5% CO_2), and the fluorescence displayed by the reduction of the dye by the metabolically active cells was recorded in a microplate reader (Multimode Synergy HT Microplate Reader; Biotek, US) at 530 nm excitation and 590 nm emission wavelengths. The viability was calculated by linear interpolation of the fluorescence data from the cells exposed to gold compounds versus the non-treated ones (control sample, 100% viability).

2.7. Cell apoptosis and cell cycle

Fibroblasts and macrophages were seeded at densities of 4×10^4 cells/well in 24-well plates and maintained at 37 °C and 5% CO_2 overnight. Fibroblasts and macrophages were then treated with the subcytotoxic concentrations of Au (III) or Au (I) obtained in the cytotoxicity assay described above. After 24 h of incubation, cell apoptosis and cell cycle were studied by flow cytometry (FACSARIA BD equipment and software).

To determine cell apoptosis, after 24 h of exposure to the different gold species concentrations, cells were harvested, resuspended in annexin V-binding buffer (10 mM HEPES/NaOH, 140 mM NaCl, 25 mM $CaCl_2$) and treated with a solution composed of annexin V-FITC and propidium iodide. Cells were then incubated at room temperature for 15 min in the dark and then analyzed by flow cytometry (FACSARIA BD equipment and software, US). Samples were analyzed in triplicate. Untreated control cells were used as a negative control to determine the basal status of the cells and comparatively with the effects of gold on macrophages and fibroblasts.

Furthermore, the distribution of the cell-cycle phases after gold exposure was assessed by flow cytometry (FACSARIA BD equipment and software, US). After 24 h of exposure to the different gold species concentrations, cells were collected and fixed with 70% ice-cold ethanol (10^6 cells/mL). DNA staining was performed by adding RNase A and propidium iodide to the cell solution. Finally, samples were analyzed by flow cytometry (FACSARIA BD equipment and software, US). Control samples (untreated cells) were also run to know the standard distribution of cell cycles in the cell lines assayed.

2.8. Immunofluorescence assay

Cells (4×10^4 cells) were seeded onto sterile coverslips and treated or not with the subcytotoxic concentrations of Au (III) or Au (I) for 24 h. Then, cells were rinsed with PBS and fixed in paraformaldehyde 4% (Alfa Aesar, Germany) during 30 min at room temperature. After fixation, cells were first washed with PBS-BSA 1% and then with saponin 0.1% in PBS-BSA solution. Afterwards, the samples were stained for 1 h at room temperature with primary antibodies against vinculin (1:200) (SAB, US) and tubulin (1:50) (Molecular Probes, US). After washing, the cells were incubated with Alexa Fluor 488 goat anti-rabbit IgG antibody (1:250) (Molecular Probes, US) for vinculin and Alexa Fluor 633 rabbit anti-mouse IgG antibody (1:250) (Molecular Probes, US) for tubulin. F-actin was labelled with Phalloidin 546 (1:200) (Molecular Probes, US) in PBS-BSA-saponin prepared solution. Then, cells were rinsed with PBS−BSA 1% and then with distilled water. Finally, coverslips were mounted on glass slides in DAPI-Mowiol mounting medium (ThermoFisher Scientific, US). Samples were visualized by confocal microscopy (Leica TCS SP2 Laser Scanning Confocal Microscope, Germany).

2.9. Mitochondrial membrane potential and ROS production

To assess whether gold species treatment modifies the mitochondrial cell membrane potential, fibroblasts and macrophages were seeded (6×10^4 cells/well; 24-well plates) for 24 h in DMEM

with 10% FBS, and then treated with subcytotoxic concentrations of Au (III) or Au (I) for 24 h. After the exposure to gold species, cells were collected and resuspended in PBS. To evaluate the mitochondrial membrane potential, 5 μL of 1,1′,3,3,3′-hexamethylindodi carbo-cyanine iodide (DilC1(5) InmunoStep, Spain) were added, incubated for 15 min at 37 °C, 5% CO_2 and then analyzed by flow cytometry (FACSARIA BD equipment and software, US).

ROS generation was indirectly evaluated by the cell-permeable CellROX® reagent (ThermoFisher Scientific, US). This compound is essentially non-fluorescent in a reduced state, but exhibits a strong fluorogenic signal upon oxidation, providing a reliable measurement of ROS generation in live cells. Fibroblasts and macrophages were treated with 62.5 μM Au (III), 125 μM Au (III), and 125 μM Au (I) for 24 h. Then, cells were collected, mixed with CellROX® reagent at 500 nM and incubated for 30–60 min at 37 °C, protected from the light. During the last 15 min of staining, 1 μL of the 5 μM SYTOX® Red Dead Cell reagent was added. Afterwards, the generation of ROS was monitored using 488/525 nm excitation/emission of the CellROX® Green by flow cytometry (FACSARIA BD equipment and software, US).

3. Results and discussion

3.1. Gold bactericidal activity

In the search for alternatives to antibiotics, we previously demonstrated promising results for gold-chitosan nanocomposites regarding their strong bactericidal effects without damaging eukaryotic cells at equivalent doses, not only in independent cell cultures, but also in *in vitro* infection models [12,21]. As we showed, chitosan by itself did not display antibacterial ability so this effect was solely attributed to Au NPs and to the gold species released from them. The present work clarifies the role of Au (III) and Au (I) species in their bactericidal effects deciphering the molecular mechanisms exerted in bacteria.

Concerning the bactericidal effects in planktonic cultures, at the doses tested (50–125 μM) Au (III) and Au (I) species showed bactericidal effect on *E. coli* whereas no effect was observed on *S. aureus* (Fig. 1A). Specifically, Au (III) displayed dose-dependent effects on *E. coli* cultures depleting bacteria growth (~10^2 CFU/mL)) at the lowest concentration assayed (50 μM) whereas the complete eradication of bacteria was achieved at the highest concentration tested (125 μM). On the other hand, Au (I) significantly inhibited bacteria growth (10^6-10^7 CFU/mL) at the concentrations assayed though a dose-dependency was less pronounced. It should be noted that the range of gold concentration was chosen regarding the results that our group obtained in previous studies [21]. Other authors have also shown similar results pointing to the higher bactericidal effects of Au (III) compared to Au (I) as well as lower minimum inhibitory concentration (MIC) values of Au (III) against *E. coli* than against *S. aureus* [22]. The evaluation of the antimicrobial ability of Au (III) against the Gram-negative bacteria *P. aeruginosa* revealed the efficiency of ionic gold as bactericidal agent displaying MIC values close to those exerted by different antibiotics. The superior antimicrobial action on Gram-negative bacteria may be attributed to the cytoderm thickness (10 nm in Gram-negative bacteria vs 20–80 nm in Gram-positive bacteria [23]), which is related to the peptidoglycan content, as well as to the hydrophilic/polar character of both forms of ionic gold. Small hydrophilic ions and drugs passively diffuse to the bacterial interior by using the pore-forming porins in Gram-negative bacteria while macrolides and other hydrophobic drugs diffuse preferentially across the lipid bilayer in Gram-positive bacteria [24]. Transporters of the general bacterial porin (GBP) superfamily control the energy-independent diffusion of polar solutes including metal ions into Gram-negative bacteria [3]. Compared to Gram-positive bacteria, the superior antimicrobial action found in Gram-negative bacteria can also be associated to their superior glutathione and soluble thiol content which are responsible for their cytoplasm reductive environment [25]. In addition to the physiological extracellular content, at cytotoxic doses, bacterial death would release additional glutathione and soluble thiol upon cell lysis, which could

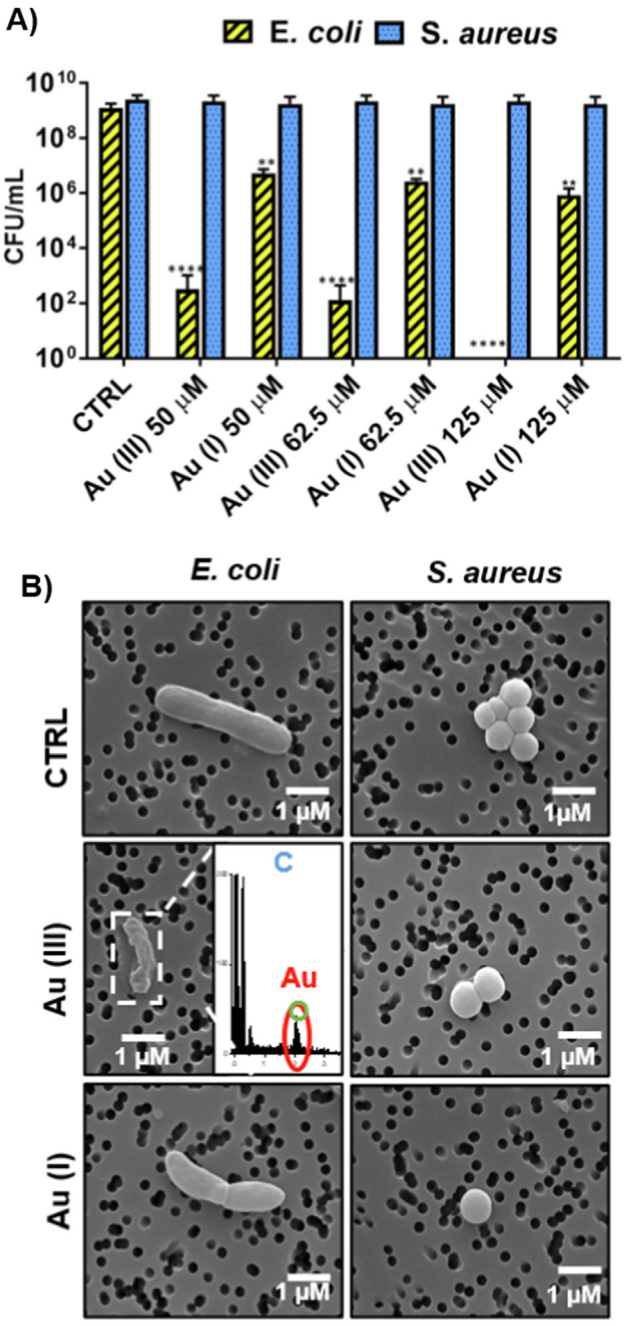

Fig. 1. Effects of Au (III) and Au (I) treatment in bacteria cultures. A) Bacteria growth (CFU/mL) obtained after treatment of *E. coli* and *S. aureus* cultures with Au (III) and Au (I) at different ionic gold concentrations (50–125 μM) for 24 h. Control samples represent *E. coli* and *S. aureus* non-treated with any gold species. Data are expressed as the mean ± SD of at least four independent experiments performed in triplicate ($n \geq 12$) and showing statistically significant differences between the control samples and the treated ones (**$p \leq 0.01$; ****$p < 0.0001$). B) Bacteria morphology observed by SEM before (Control samples) and after treatment with Au (III) or Au (I) at 125 μM except for Au (III) in *E. coli* cultures where the gold precursor was added at 50 μM concentration. EDX spectrum is also depicted to corroborate the presence of gold. Note: EDX analysis did not reveal the gold presence for Au (I)-treated bacteria in any of the areas scanned.

contribute to reduce larger amounts of available gold species into metallic gold. Therefore, detoxification red-ox reactions would be promoted in Gram-negative bacteria. In agreement with the previous literature, higher concentrations of Au (III) and Au (I) are needed to eliminate Gram-positive bacteria compared to Gram-negative ones and a superior antimicrobial action of Au (III) vs Au (I) was also observed [26]. The largest inhibition of bacterial growth was observed after treatment with Au (III) concentrations above 125 μM on *E. coli* under aerobic conditions which was attributed to the unbalance of the bacterium's oxidative status [10]. The superior antimicrobial action of Au (III) vs Au (I) found can be attributed to the higher reduction potential of Au (I) (1.83 v) compared to that of $[AuCl_4]^-$ (0.93 v) and therefore a superior tendency to participate in oxidative reactions for the latter. We hypothesized that Au (III) could be easily reduced in culture to Au (I) whereas Au (I) is reduced to zerovalent inert Au (0) which would be in agreement with the superior toxicity observed for Au (III). This hypothesis was validated later on thanks to our XPS results (see subsequent section). Also, compared to Au (I), Au (III) has a higher positive charge and therefore is a harder acid that can easily form complexes with different harder bases being more reactive. Considering these previous works and the differences found in our assays, different methodologies were performed to elucidate cellular and molecular mechanisms involved in the toxicity of those gold species against prokaryotic cells and whether these effects were also found in eukaryotic cells.

3.2. First mechanism of antimicrobial action: Cell wall damage

Fig. 1B depicts characteristic morphological changes on bacteria observed by SEM after treatment with ionic gold. Untreated controls showed the characteristic elongated morphology of coliform bacteria (*E. coli*) prepared for cell division and the characteristic clustered growth of *S. aureus* cocci. After Au (III) treatment, severe cell damage was observed for *E. coli* on its cell wall showing a crumpled structure probably attributed to cell lysis while the surface and morphology of *S. aureus* remained unaltered. On the other hand, when bacteria were treated with Au (I), *E. coli* surface showed increased roughness and some pinholes were present whereas no changes were observed for *S. aureus*. It should be noted that *E. coli* was treated with a lower Au (III) concentration as at the highest concentration assayed (125 μM), bacteria were totally eradicated and it was not possible to study their morphology. The shrunk structure observed in Au (III)-treated *E. coli* samples agrees with previous morphological studies where a size reduction is clearly observed when *E. coli* was treated with $HAuCl_4$ for biomineralization induction [27]. Furthermore, EDX analysis revealed the presence of gold on Au (III) treated bacteria (Fig. 1B). Those morphological changes are in accordance with the bactericidal results explained above (Fig. 1A) and can be attributed to the cell wall destabilization caused by Au (III).

The optical resolution of SEM was insufficient to elucidate whether reduced metallic Au NPs were formed and responsible for the gold signal retrieved from the EDX analysis. Therefore, ultramicrotomed slices of bacteria were observed under TEM to identify their presence (Fig. 2). It should be noted that, in order to properly visualize bacteria, *E. coli* samples were treated at lower concentrations (62.5 μM) than *S. aureus* cultures (125 μM) due to the higher cytotoxicity exerted by gold species (Fig. 1A). Bacteria produce extracellular substances (ECS) which are able to modify the size and zeta potential of NPs by causing their agglomeration, thus preventing them from having contact with the bacteria and decreasing their bactericidal activity [28,29]. Fig. 2A1 and 2A2 show that Au NPs were formed in the close proximity of *E. coli* and *S. aureus*, respectively. Under the conditions tested, no isolated Au NPs were observed in the extracellular medium of *E. coli* (Fig. 2A1) which might indicate that at the concentrations used the polysaccharides, metal chelating compounds (i.e., siderophores), and proteins secreted by these bacteria were insufficient to reduce bioavailable soluble gold species. Probably most of the reduction takes place only on the external surface of *E. coli* due to the reductive character of the hemiacetal groups present on the cell surface saccharides as previously reported [18]. Also, because the exposure doses were below the corresponding MBCs, the release to the extracellular milieu of large amounts of the bacterial intracellular content was not expected, which could have been responsible for strong metal-reductive conditions outside the cells. TEM images (Fig. 2A2) of *S. aureus* treated with Au species also showed the uneven presence of 9.5 ± 4.5 nm Au NPs on the surface of bacteria. Again, no NPs were observed in the extracellular space (Fig. 2A2). Large nanoparticle aggregates (size ranging from 500 nm to 2 μm) were observed for both Au (III) and Au (I) treated samples, probably as part of a bacteria-driven detoxification process.

The interaction between Au (III) and Au (I) cations with the cell membrane was also corroborated by FTIR analysis. Fig. 3A shows that no changes in the spectra could be observed when comparing the spectra of *S. aureus* bacteria treated with Au (III) or Au (I) and the untreated ones. On the other hand, observed changes in the corresponding spectra suggest that different supramolecular interactions appear when treating *E. coli* with those ionic gold species. Spectrum of bacteria treated with Au (III) (Fig. 3A) shows modifications in the bands related to amide I (1600–1800 cm^{-1}) and amide II (1470–1570 cm^{-1}) vibrations, the main bands of proteins in the IR spectrum. Amide I absorption band at 1637 cm^{-1} has been previously assigned to the stretching vibrations of the C═O groups at β-pleated sheet structures in proteins [30] which could be associated to the lipoprotein (Lpp) which crosslinks the outer membrane and the inner peptidoglycan layer of *E. coli* regulating the mechanical properties of its envelope [31]. After contacting with Au (III), a slight shift in the amide I band to lower wavenumbers was observed, which could indicate a structural interaction with the β-sheets of cell membrane proteins, whereas no shift was observed for bacteria in contact with Au (I) at the concentration tested. A shift was also observed for the amide II band (1540 cm^{-1}). This signal has been previously assigned to the high α-helical content of membrane proteins in *E. coli* [32]. As a result of the Au (III) and Au (I) treatment, the amide I and II bands were shifted to lower wavenumbers thus demonstrating alteration in the protein structures possibly due to the lysis of the cell membrane [33]. A new peak appeared at 1587 cm^{-1} in the treated *E. coli* which could be associated to a metal-nitrogen bond formation [34]. This may be also supportive of the lysis of the cell membrane. The IR band at 1396 cm^{-1} has been previously attributed to the symmetric CH_3 bending of the methyl groups in proteins [35,36] and again a shift was observed in the spectra when interacting with both gold species. A new peak appeared at 1300 cm^{-1} in the treated *E. coli* which may indicate again a possible Au-N interaction [37]. A slight shift in the 1240 cm^{-1} peak was observed after treatment with Au (III) and Au (I). According to the literature, the region between 1500 and 1200 cm^{-1} is governed by the vibrational signals of proteins, fatty acids, and phosphate bearing compounds [33]. After contacting with Au (III) and Au (I), a slight shift in the 1070 cm^{-1} peak to lower wavenumbers was also noted in the treated cells, this band corresponds to (C — O – C) stretching vibrations of the bacterial membrane glycosidic linkages [33]. Hence, FTIR spectra suggested that for *E. coli,* the treatment with Au (III) and Au (I) causes the destruction of the cell membrane by the alteration in its protein structure revealed by the shifting in the amide I and II bands, by the appearance of new absorption bands depicting possible destruction of membrane phospholipids, and by the breakdown of glycoside linkages of the polysaccharides present in the

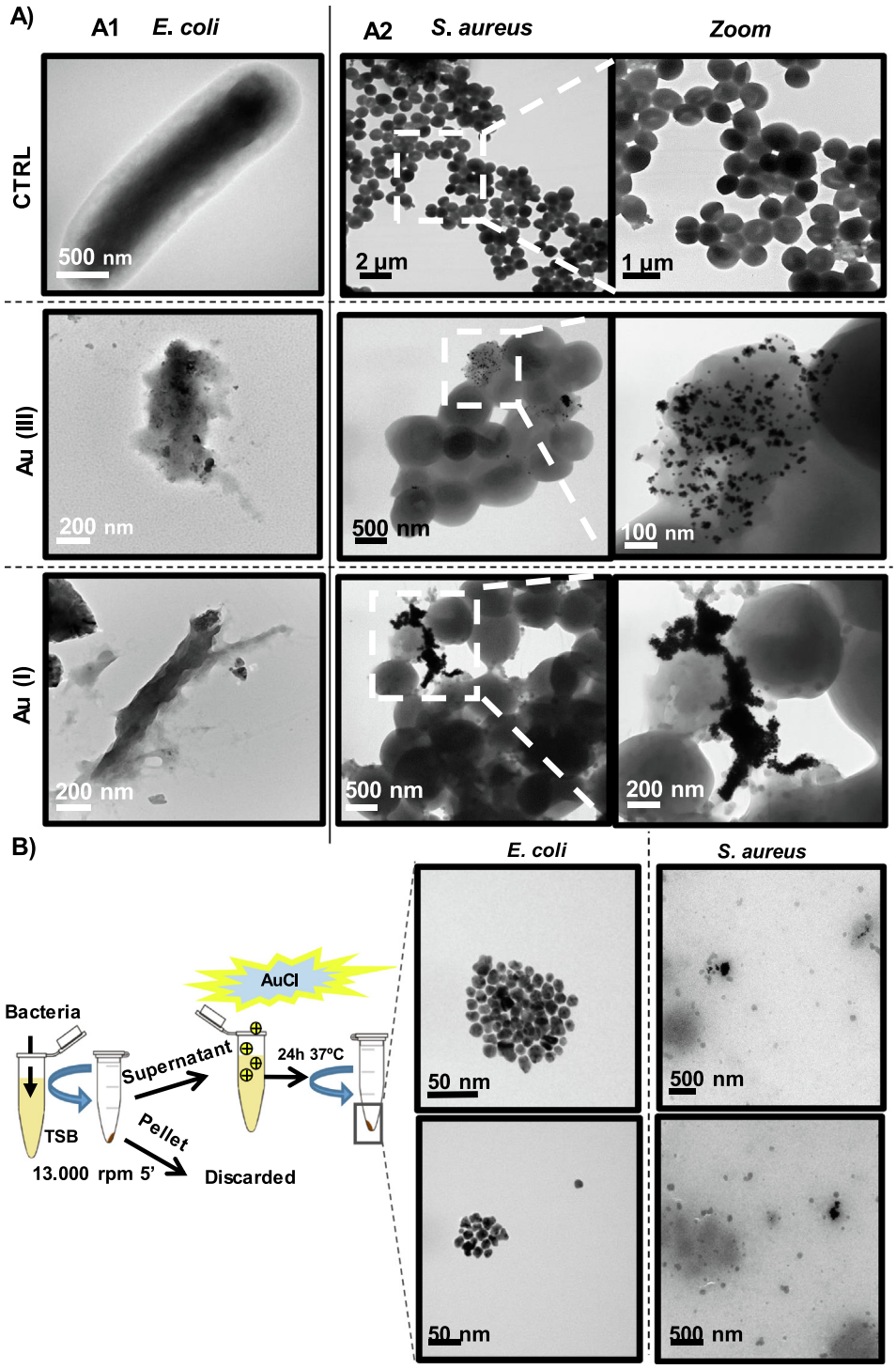

Fig. 2. TEM micrographs of bacteria treated with ionic gold species and consequent Au NPs formation. A) Bacteria treated with gold species. A1) *E. coli* and A2) *S. aureus* before (control sample) and after treatment with Au (III) or Au (I) for 24 h. *E. coli* was treated with 62.5 µM of both gold species whereas *S. aureus* with 125 µM concentration of both gold precursors. Right images correspond with a zoomed area of the middle images. B) *In vitro* synthesized Au NPs by *E. coli* (left) and *S. aureus* (right) crude extracts (i.e., exudates) after treatment with 125 µM Au (I).

cell membrane. In summary, gold species cause *E. coli* membrane damage which would interfere in its membrane potential and would contribute to intracellular components leakage.

3.3. Second mechanism of antimicrobial action: Oxidative stress induction

XPS results on Au (III) and Au (I) treated bacteria corroborated the presence of intracellular gold after surface etching (Fig. 3B). Interestingly, when Au (III) was added to bacteria, it was reduced to Au (I) in both the external surface (etching time 0 s) and internally (etching 200 s). No Au (III) was detected after contacting with both bacteria. Supporting the antimicrobial results (Fig. 1), it was observed that against *E. coli*, Au (III) remained in ionic form (as Au (I)). However, against *S. aureus*, all the Au (III) added was reduced to zerovalent Au on the surface of the cell, obtaining Au NPs as it was observed in the TEM micrographs (Fig. 2A2), which could explain its reduced cytotoxicity against these Gram-

A)

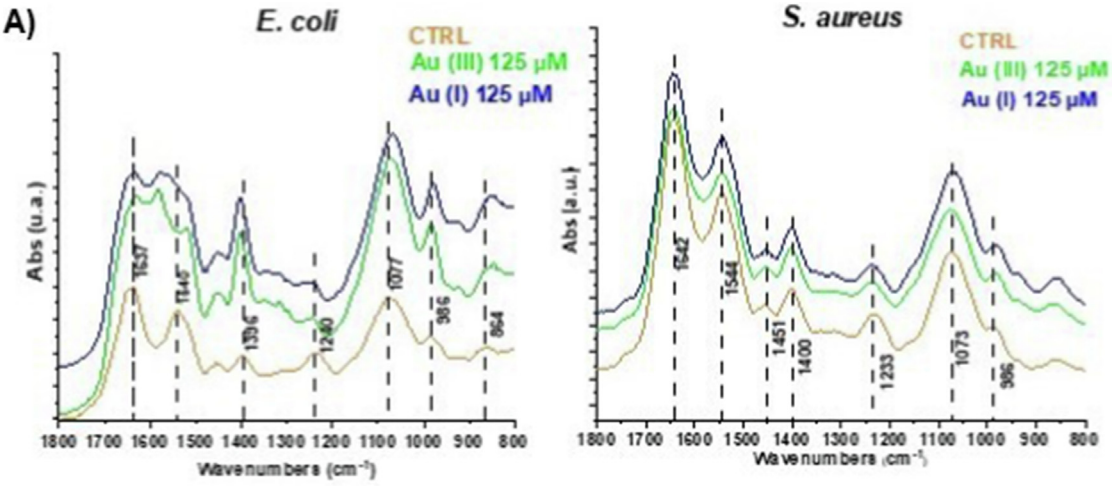

B)

E. coli	Etching (s)	B.E. (eV) Atomic % Au (0)	Au (I)	Au (III)
Au (III) 62,5 µM	0		85.0 100%	
	200		85.4 100%	
Au (I) 50 µM	0	83.8 100%		
	200	83.9 69%%	84.9 31%	
Au (I) 125 µM	0	83.5 100%		
	200	83.9 67%	85.4 33%	

S. aureus	Etching (s)	B.E. (eV) Atomic % Au (0)	Au (I)	Au (III)
Au (III) 125 µM	0	83.9 100%		
	200	83.9 43%	85.5 57%	
Au (I) 50 µM	0	83.7 100%		
	200	83.7 23%	85.3 77%	
Au (I) 125µM	0	83.9 100%		
	200	84.0 33%	85.5 67%	

C)

D)

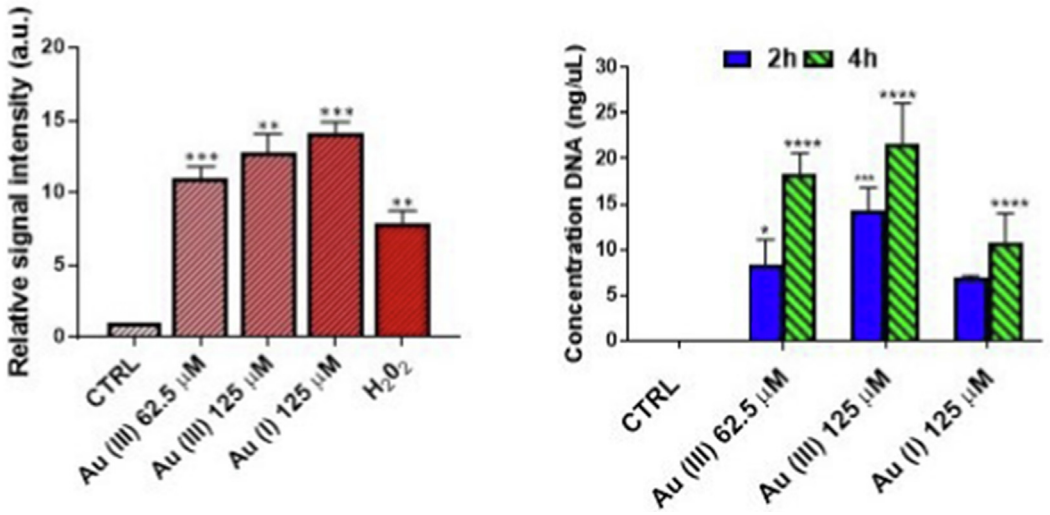

Fig. 3. Effects of gold species in the bacteria wall, ROS generation and DNA integrity. A) FTIR spectra of *E. coli* and *S. aureus* cell mass after 24 h treatment with Au (III) or Au (I) at a concentration of 125 µM. B) Concentration of gold species (atomic wt.%) determined by XPS after bacteria treatment. C) Quantitative levels of ROS in *E. coli* exposed to the different gold species concentrations. Data are expressed as fluorescence intensity levels relative to those obtained for the untreated controls (control value assigned as 1). D) Concentration of nucleic acids released from bacteria after 2 and 4 h of incubation with Au (III) 62.5 µM, Au (III) 125 µM and Au (I) 125 µM. Data are expressed as mean ± SD of at least 3 independent experiments performed in triplicate. Statistically significant differences between the control samples and the treated ones (* $p < 0.05$; ** $p < 0.01$; *** $p < 0.001$; **** $p < 0.0001$) are also depicted.

positive bacteria. After etching, partially oxidized Au (I) (57 at. %) was detected intracellularly and 63 at. % as Au (0) on the surface. When Au (I) was added to *E. coli*, only Au (0) was detected on the surface of the bacteria and after etching, both Au (0) and Au (I) were detected intracellularly. This fact may explain the reduced toxicity observed for Au (I), which in presence of bacteria can be reduced to Au (0) decreasing its potential cytotoxicity, whereas Au (III) remains reduced as Au (I) maintaining its cytotoxic effect.

As it is shown in the SEM images (Fig. 1B), the interaction of *E. coli* with gold species resulted in the disruption of the bacterial cell wall through the formation of perforations which eventually resulted into a complete cell lysis (Fig. 2A) in agreement with the previous literature [38].

Both bacteria were able to biomineralize gold species but despite of the fact that some metallic NPs were found on Au (III)-treated *E. coli* (Fig. 2A), probably most of the Au remains in its ionic soluble form (as reduced Au (I)) as XPS results corroborated (Fig. 3B). This is based on the fact that while TEM is a local morpho-analytical technique, XPS analysis gives macroscopic information as it was carried out in 1 mm^2 sections of treated bacteria.

Moreover, exudates released by bacteria were used to analyze the potential reductive induction caused by the extracellular components and the culture medium and to evaluate the potential extracellular Au (0) formation before contacting bacteria. No nanoparticles were found when Au (III) precursor was mixed with those exudates under the same experimental conditions than the ones used when culturing bacteria. However, when the Au (I) precursor was added to the culture medium containing all bacterial exudates, 23 ± 6 nm Au NPs were detected in the medium used for *E. coli* growth after 24 h of incubation (Fig. 2B). Potentially in the culture medium containing bacterial exudates, Au (III) species were reduced to monovalent ionic form whereas Au (I) was reduced to its metallic zerovalent form. It has been reported that Au (III) species are not stable in aqueous conditions and undergo spontaneous hydrolysis [39]. Depending on the presence of different nucleophiles and reductors in the media, Au (III) can be reduced to Au (I) according to the electrochemical half reaction (Equation (1)):

$$Au^{3+}+2e^{-}\rightarrow Au^{+},\ E^{0}=1.29V \quad (1)$$

Those results were corroborated by UV–VIS spectroscopy analyzing the extinction spectra of both precursors dissolved in the culture medium (TSB). Figure S1 shows that, at the concentrations used in this work, no extinction peaks at 520 nm characteristic of the surface plasmon resonance of solid spherical Au (0) NPs were formed, but by increasing the precursor concentration to 10 mM, the characteristic localized surface plasmon resonance peak was observed when Au (I) was used but no peak was detected under the same conditions when Au (III) was used. Probably at the low concentrations used in this work the extinction spectra cannot reveal Au NPs formation due to their reduced size and concentration, but NPs are formed when using Au (I) as precursor as we corroborated by TEM. It has been theoretically and experimentally demonstrated that the reduced mean free path of the conduction electrons in small particles is responsible for their lack of surface plasmon resonance (SPR) bands [40]. For Au NPs with sizes less than 10 nm, SPR bands are largely hindered due to the phase changes resulting from the increased rate of electron-surface collisions compared to those of larger particles [41].

Concerning the different effects observed in the above-described experiments regarding Gram-positive and Gram-negative bacteria, all assays from this point were only performed in the Gram-negative bacteria model, *E. coli*, due to the lack of antimicrobial effect against Gram-positive bacteria observed at the doses tested.

To validate the different reductive character of Au (III) and Au (I), *in vitro* ROS generation using the DHR123 probe, which is an uncharged and non-fluorescent ROS probe that becomes fluorescent under the presence of peroxynitrite and other ROS [42], was analyzed. Under the presence of *E. coli*, both Au (III) and Au (I) species generated ROS in significant amounts compared to the basal status of the cells (Fig. 3C) resulting in oxidative damage. No statistically significant differences were found in the amount of ROS generated in both species at the same concentration. Therefore, the superior bacterial damage observed for Au (III) on *E. coli* cannot be solely attributed to ROS generation. In summary, both Au (III) and Au (I) are able to induce oxidative stress on *E. coli* bacteria. This oxidative effect was later corroborated by means of genomic and proteomic analyses (see subsequent sections).

3.4. Third mechanism of antimicrobial action: Nucleic acid release and DNA damage

Previous studies showed that gold clusters and Au (III) complexes bind to DNA and cause its damage [43]. Also, the high levels of ROS production results in the degradation of the genetic material [44]. As shown in Fig. 3D, the exposure of *E. coli* to Au (III) and Au (I) for 2 h produced a large amount of nucleic acids release which is proportional to the measured bactericidal effect shown above (Fig. 1A). After 4 h of contact, the amount of nucleic acids released significantly increased and Au (III) 125 μM produced the highest nucleic acid release at both time points. These results confirm the dose- and time-dependent bactericidal effect as well as the damage exerted to the bacterial cell wall in the presence of gold species facilitating the release of nucleic acids to the extracellular space.

3.5. Fourth mechanism of antimicrobial action: Genetic response to oxidative stress

Owing to the bactericidal effect of Au (III) and Au (I) species, the antioxidant response at molecular level to those stressors was evaluated in *E. coli* in a late exponential phase (10^7 CFU/mL) by RT-PCR (Fig. 4A). As explained above, genes corresponding to stress responses (*oxyR, rpoS, sodA*) and two thiol-disulfide oxidoreductases (*grxA, trxA*) were analyzed whereas gene expression was normalized to the level of *gapA* (Table S1). It should be noted that the assays were performed by treating *E. coli* with Au (III) at 62.5 μM and Au (I) at 125 μM. Au (I) 125 μM was selected for further experiments being the MIC for the compound and Au (III) 62.5 μM (half MBC) was selected for further experiments because at 125 μM Au (III) the MBC was reached (Fig. 1A) and no remaining bacteria was left. The gene expression analysis (Fig. 4A) showed a significant induction of *rpoS* (3.07-fold), *grxA* (2.96-fold) and *sodA* (2.91-fold) genes after treatment with Au (III) at a concentration of 62.5 μM, whereas only rpoS (2.95-fold) and *grxA* (2.55-fold) gene expressions were significantly increased after exposure to Au (I) 125 μM. *RpoS*, a sigma subunit of RNA polymerase, has been reported as the main regulator of the general stress response in *E. coli* [45]. Its expression was increased after treatment with both gold species, thus indicating that the activation of rpoS regulon may help *E. coli* to protect itself from any unbalance in the bacterium's oxidative status. In addition to the glutathione system, *E. coli* contains thiol-disulfide oxidoreductases that maintain the thiol-disulfide balance in the cytoplasm [46]. Though *trxA* and *grxA* encode cytoplasmic disulfide reducing proteins (thioredoxins and glutaredoxins), only Au (III) 62.5 μM and Au (I) 125 μM triggered a *grxA*-dependent response, which seems to indicate that the glutaredoxin system is more sensitive to this redox unbalance than

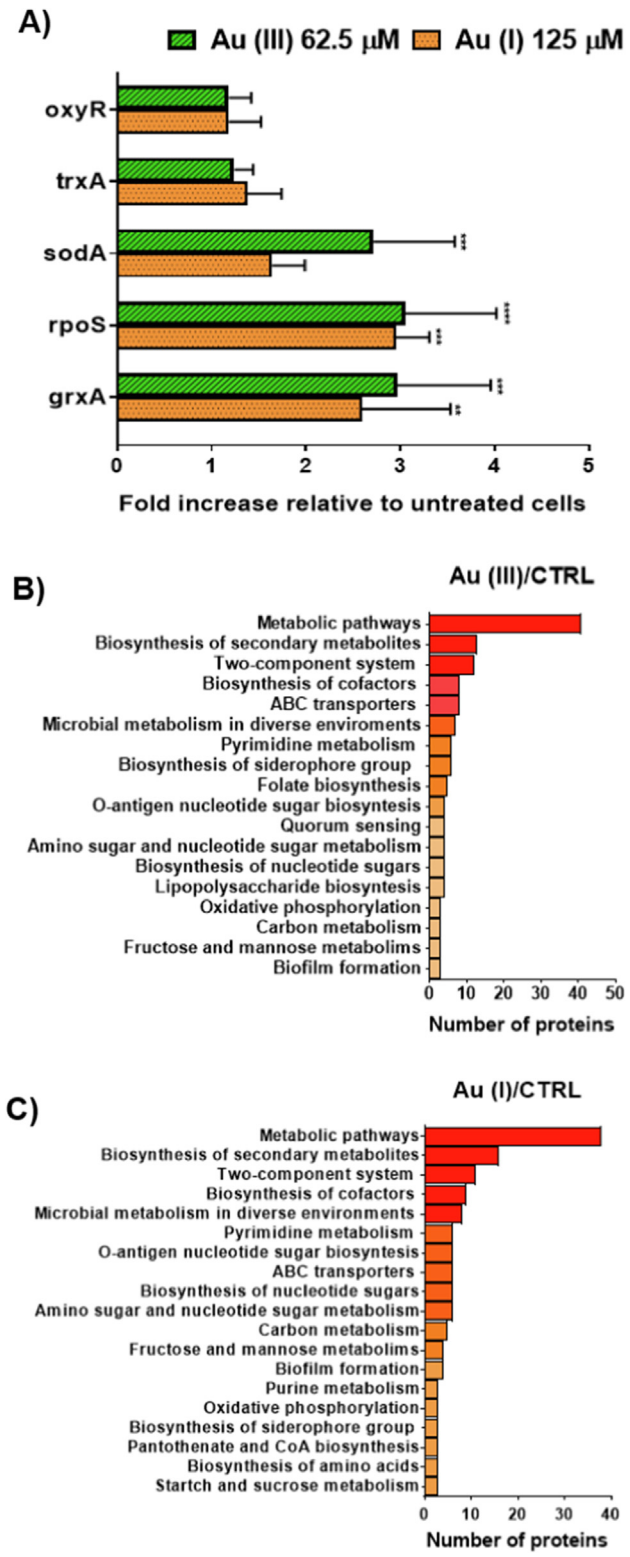

Fig. 4. Effects of gold species at the molecular level in *E. coli*. A) Genetic response after treatment with Au (III) 62.5 µM or Au (I) 125 µM. The fluorescence signal of each PCR product was compared to that of *gapA*. The values obtained from tested genes were normalized to those obtained from control groups (non-treated cells). B) Proteomic analysis after treatment with Au (III) 62.5 µM: KEGG pathway enrichment analysis of differentially abundant proteins of *E. coli*. C) Proteomic analysis after treatment with Au (I) 125 µM: KEGG pathway enrichment analysis of differentially abundant proteins of *E. coli*. Data are expressed as mean ± SD of at least 3 independent experiments performed in triplicate and showed statistically significant differences between the control samples and the treated ones (**p < 0.01;***p < 0.001; ****p < 0.0001).

the thioredoxin system. Since sodA activates a group of enzymes that attenuate the effects of superoxide, only Au (III) at 62.5 µM triggered a *sodA*-dependent response. These results support the higher capacity of Au (III) species to trigger the unbalance of the bacterium's oxidative status [10]. The expression of the transcriptional factor *oxyR*, that is oxidized by hydrogen peroxide through the formation of an intramolecular disulfide bond [47], was not increased after the 125 µM treatment with any of the gold species. These results may indicate that gold species do not trigger a H_2O_2 increase high enough to reach stressing levels. In accordance with previous studies, when *E. coli* was stimulated by hydrogen peroxide, transcription of *sodA* and *rpoS* was activated in stationary phase whereas *oxyR* expression was activated during exponential growth. Additionally, the expression of *trxA* was not increased either by oxidative stress or by a shift to high-osmolarity conditions as previously reported [47].

3.6. Fifth mechanism of antimicrobial action: Gold species affect the expressed levels of target proteins

In order to decipher the effects of ionic gold treatment in protein expression, *E. coli* bacteria suspensions were treated with Au (III) 62.5 µM or Au (I) 125 µM for 2 h and analyzed by LC-MS/MS. Again, Au (I) 125 µM was selected as MIC whereas Au (III) 62.5 µM (half MBC) was also selected for those proteomic assays because, as we mentioned before, Au (III) at 125 µM elicited total bacterial elimination.

The analysis of the global proteome of *E. coli* after treatment with Au (III) and Au (I) species yielded a large amount of relevant results (Fig. 4B, 4C and S2). The different proteins showing increased abundance related to control samples are depicted in Fig. S2A. The details of differentially abundant proteins among Au (III) and Au (I) vs control sample are also detailed in the Supporting Information section (Figure S2). Gene Ontology analysis regarding biological processes, cellular locations and molecular functions that are affected after Au (III) and Au (I) treatments are depicted in Fig. S2B and S2C.

KEGG pathway analysis was performed to determine the biological pathways involved in the differentially abundant proteins detected in *E. coli* after ionic gold treatment. Pathways including only one or two proteins were omitted in the analysis. As shown in Fig. 4B and 4C, the pathways affected were directly involved with the bacterial metabolism, transport and biosynthesis. Au (III) and Au (I) action modified the biosynthesis of the cofactor pathways, thus impairing the redox homeostasis and energy metabolism in *E. coli* [48]. The molybdopterin biosynthesis, reported to be essential for *E. coli* virulence [49], and the biosynthesis of the NAD + cofactor, were only decreased by Au (III) treatment. Moreover, Au (III) showed a higher ability to trigger the *quorum sensing* and siderophore enterobactin biosynthesis pathways. The stress response was also modified after both treatments. Interestingly, 5-oxoprolinase subunit A, implicated in the first step of glutathione biosynthesis, was only increased after Au (III) treatment, thus modifying the glutathione levels upon Au (III)-induced oxidative stress and cell damage [50]. These results are in agreement with those obtained at mRNA levels. The NADH oxidoreductases were strongly down-regulated after both treatments, thus impairing the aerobic respiration in *E. coli.* Interestingly, only the c subunit of the FO ATP synthase was down-regulated after Au (I) treatment, thus suggesting that ATP synthase is mainly a target for Au (I) treatment and leading to a general decline in the cellular metabolism [51,52]. Other authors also determined that gold NPs exert their antibacterial action by changing the membrane potential and inhibiting ATP synthase [13]. Proteins involved in the two-component system EnvZ/OmpR and CusS/CusR were only affected after Au (I) treatment. The EnvZ/OmpR system is the main regula-

tor of porins [53]; a lower expression of outer membrane porin OmpC could lead to a lower intracellular accumulation of Au (I) thus conferring *E.coli* resistance to Au (I). On the other hand, CusS/CusR proteins and the zinc resistance-associated protein, known to regulate copper, silver and zinc ions homeostasis [54,55], were up-regulated. All of these findings could indicate that *E. coli* is trying to countereffect the unbalance in its homeostasis caused by Au (I) thought several mechanisms: (1) efflux system through the transmembrane transport; (2) reducing its transport into the periplasmic space via changes in its porins; (3) secretion of extracellular substances. These results could explain the lower toxicity found after Au (I) treatment.

Most proteins involved in pyrimidine and purine catabolism were increased after both treatments, thus indicating that *E. coli* is trying to overcome the gold-induced DNA damage, corroborating our previous findings in which DNA release and damage were quantified. ABC transporters pathway was also modified by the action of ionic gold, which could lead to a disorder in the transport system, homeostasis, and composition of the cell membrane. These results agree with those obtained by FTIR analysis in which, gold species caused the destruction of the cell membrane by the alteration of its protein structure. As a result of gold species action, all differentially expressed proteins involved in fructose and mannose biosynthesis, O-Antigen nucleotide sugar biosynthesis, amino sugar and nucleotide sugar biosynthesis and lipopolysaccharide biosynthesis were up-regulated. These changes could indicate that *E. coli* is trying to overcome the gold-induced lysis in the cellular membrane.

To sum up, our studies point to five different molecular mechanisms (Fig. 5) involved in *E. coli* damage mediated by gold species at the concentrations tested: cell wall damage, oxidative stress induction, nucleic acid release and DNA damage, genetic response to oxidative stress, and changes in the proteomic profile. These mechanisms resulted in bacterial death and highlight the potential of gold species as efficient bactericidal materials.

3.7. Cytotoxicity against eukaryotic cells

Two human cell lines were selected to evaluate the cytotoxic dose-response of Au (III) and Au (I) species: fibroblasts and macrophages. THP1 human monocytes (differentiated to macrophages) and human fibroblasts were chosen as cell lines based on the analysis of two main cell lineages of varied origins: somatic cells (fibroblasts) and immune system cells or professional phagocytes (macrophages). The results are depicted in Figure 6, S3, S4 and S5. As shown in Fig. 6A and according to ISO 10993–5 (Biological evaluation of medical devices: Tests for *in vitro* cytotoxicity [56]), Au (III) was not cytotoxic on fibroblasts up to 62.5 μM whereas at a concentration of 250 μM exerted a clear dose-cytotoxic response reducing the cellular viability to less than 20%. On the other hand, Au (I) displayed on fibroblasts superior viability (≥80%) at the doses tested. The higher cytotoxicity of Au (III) compared to that exerted by Au (I) has also been reported for several gold complexes bearing benzimidazole- and pyrazole-derived *N*-heterocyclic carbenes [57]. On macrophages, both gold species exerted similar viability percentages (around 70%) which could be explained by the superior plasticity of macrophages which are able to adapt to environmental stressors easily. Compared to *E. coli* viability assays (Fig. 1A), gold species were safer to eukaryotic cells at the concentrations tested, highlighting the potential of these species to treat infections without damaging human tissues. In accordance with the literature, gold nanospheres (10–40 μg/mL) [58] and Au NPs (0.1–100 μg/mL) [59] were found nontoxic to macrophages. On fibroblasts, Au (III) species triggered a reduction of 70–80% viability of cells at the highest concentrations tested (125 and 250 μM, respectively), whereas Au (I) concentrations were safer, yielding at the doses tested >80% viability. These results are in accordance with a previous study in murine fibroblasts (L929) in which Au (III) reduced viability in 80% of cells at the highest concentration evaluated (50 μg/L = 130 μM), affecting ROS production and DNA integrity [60]. Au (III) toxicity was attributed to its redox reactions with peptides and proteins, especially with sulfur-containing amino acids, and due to its ability to bind and deprotonate peptide amide bonds and cross-link histidine imidazole rings [61]. Drescher et al. [62] showed, by using laser ablation inductively coupled plasma mass spectrometry and radioactively labelled $HAuCl_4$, that $^{197}Au^+$ accumulates inside the whole cell (using mouse 3 T3 fibroblasts) and preferentially in their nuclei even generating NPs in their interior when PBS was used as culture medium but when DMEM was employed, Au NPs were formed

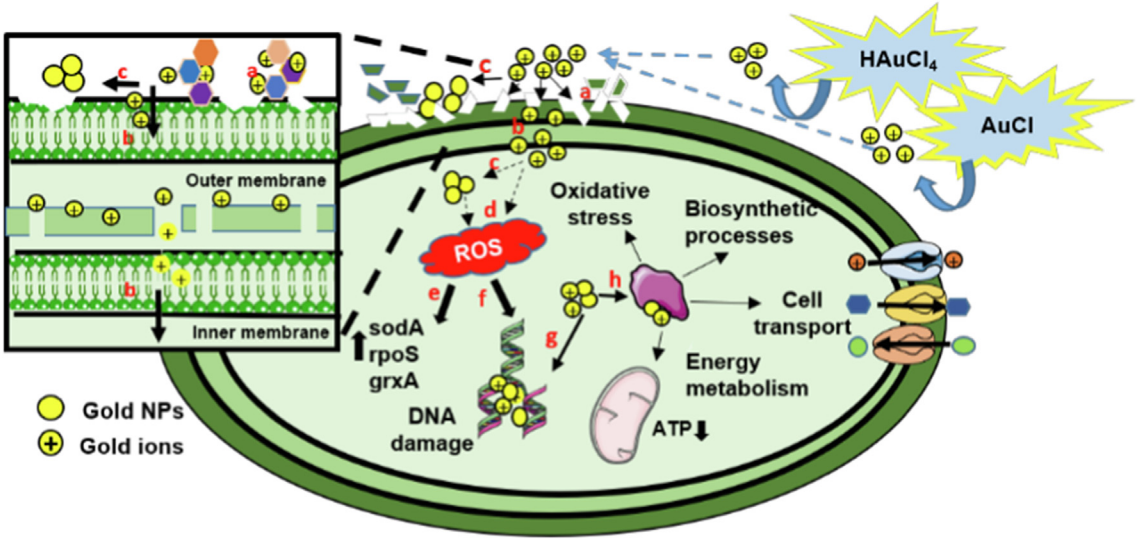

Fig. 5. Identified antibacterial mechanisms of gold species in *E. coli*. A) Positively charged gold ions electrostatically interact with the negatively-charged membrane, thus inducing bacteria wall damage. B) Passive diffusion of gold ions through the membrane. C) Formation of Au NPs during the reductive biomineralization process in both intra and extracellular spaces. D) The accumulation of Au NPs and gold ions disrupt the intracellular balance, resulting in ROS production and oxidative stress. E) Genetic response to gold-induced oxidative stress. F) DNA damage mediated by ROS. G) Gold species damage DNA. H) Gold species affect target proteins mainly involved in oxidative stress, biosynthetic processes, cell transport, and bacterial energetic metabolism.

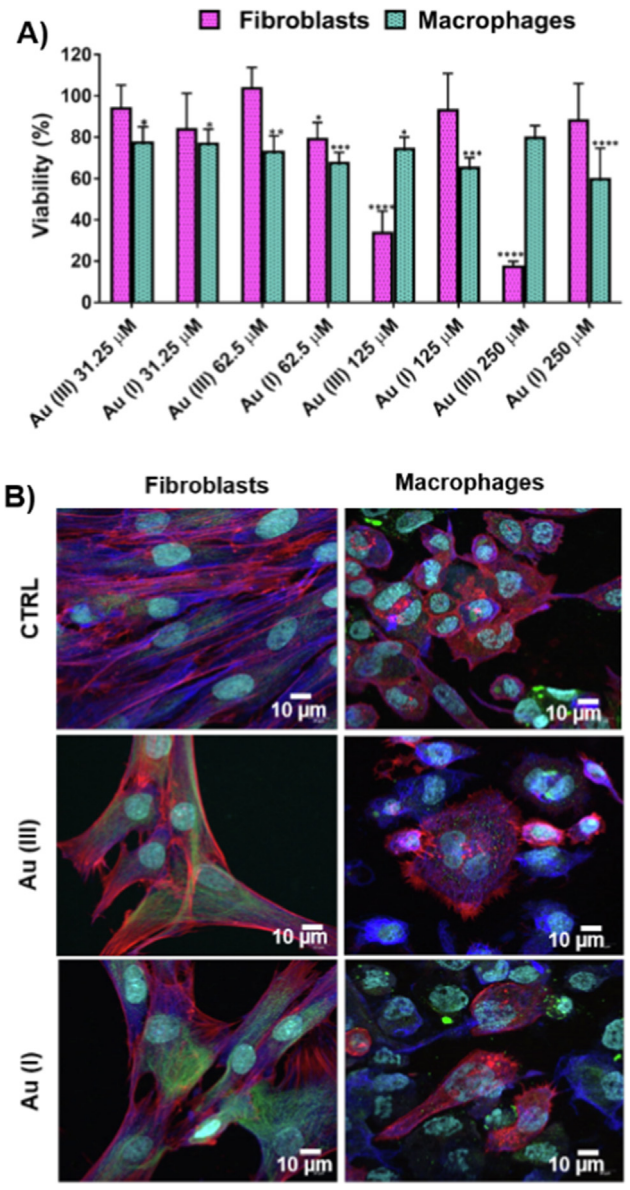

Fig. 6. Effects of gold species treatment in human cell cultures. A) Cell viability after treatment with different Au (III) and Au (I) concentrations for 24 h. Data are expressed as mean ± SD of at least 3 independent experiments performed in triplicate and showed statistically significant differences between the control samples and the treated ones (*$p \leq 0.05$; **$p \leq 0.01$; ***$p \leq 0.001$; ****$p \leq 0.0001$). B) Representative confocal images of cells before (control samples) and after treatment with Au (III) at 62.5 µM and Au (I) at 125 µM on fibroblasts and at 125 µM of Au (III) and Au (I) on macrophages for 24 h. Merged images of actin staining (red), tubulin (blue) and vinculin (green) are depicted. Scale bars: 10 µm. (For interpretation of the references to colour in this figure legend, the reader is referred to the web version of this article.)

already in the extracellular space and then internalized to their interior.

In the flow cytometry and immunofluorescence assays, macrophages and fibroblasts were treated with the subcytotoxic concentrations for Au (III) and Au (I) species and also according to the antibacterial studies, as depicted in Fig. 6B, S3, S4 and S5. Apoptosis (Fig. S3A) was determined by using Annexin V-FITC/Propidium Iodide (PI) through flow cytometry. Au (III) at a concentration of 62.5 µM and Au (I) at 125 µM were chosen due to their high bactericidal efficiency in *E. coli* while maintaining high viability percentages in fibroblasts (>94%), not observing significant changes in apoptosis nor necrosis. The macrophages treated with 125 µM of Au (III) and Au (I) maintained high viability percentages (>82%). At these bactericidal and inhibitory concentrations, no significant increase was observed in the total apoptotic response (<6%) neither necrotic effects as other authors have previously shown [59]. In this previous study, AuNPs did not reveal cytotoxic nor inflammatory responses in murine macrophages after treatment with Au NPs (0.1–100 µg/mL). On the other hand, cell cycle status (Fig. S3B) was also analyzed after treating fibroblasts and macrophages with the ionic gold species for 24 h at the same conditions described in the apoptosis assays. In this regard, no significant changes (<10%) in cell cycle phases distribution were obtained in both cells compared to control (untreated) cells. To sum up, flow cytometry studies confirmed cell viability results depicted in Fig. 6A and highlighted the low toxicity of the gold species tested on human cells at the doses of study.

To analyze whether the bactericidal ionic gold concentrations affected cell morphology in fibroblasts and macrophages cultures, changes in cytoskeleton and cell spreading were studied by immunofluorescence. Confocal microscopy images (Fig. 6B and S4) showed that cell membrane of both cell types was not disrupted after being incubated with subcytotoxic concentrations of Au (III) and Au (I). The intact structure of the cell membrane is vital for maintaining the functional integrity of mammalian cells. On the basis of these images, no effects on cytoskeleton distribution were observed for both cell types exposed to subcytotoxic concentrations of Au (III) and Au (I), with a clear maintenance of actin and tubulin architectures, as indicated by the fluorescently-labeled phalloidin (red) and tubulin network staining (blue). In addition to these findings, no effects were observable on focal adhesions compared to the control samples, as can be observed by the highly intense vinculin staining (green) localized preferably where several actin fibers merged.

Therefore, cytotoxicity appears to be dependent on the speciation state of gold (e.g., Au (III) or Au (I)) and its concentration, the cell line tested and the culture medium composition, and also in the natural biogenesis of gold NPs in the cells, as other authors have previously shown when using RPMI 1640 or DMEM culture media containing FBS with the additional aggregation induction of the formed Au NPs [62].

Finally, the mitochondrial membrane potential was analyzed in order to test the possible interactions of ionic gold with the mitochondrial function in both cell lines (Fig. S5A). The mitochondrial membrane potential was found to be altered in both fibroblasts and macrophages after contacting with gold species and, at 125 µM, affecting more to fibroblasts treated with Au (III) than those treated with Au (I), which correlates with the viability results (Fig. 6A). However, the mitochondrial membrane potential exerted by fibroblasts remained unaltered when treated with Au (I) at 125 µM, though it was strongly affected when macrophages were treated at the same concentrations. Moreover, ROS production (Fig. S5B) was also evaluated *in vitro* for both cell lines revealing oxidative stress mediated by both species. Even though no direct correlation among cell viability and apoptosis, cell morphology and focal adhesions, mitochondrial membrane potential and ROS generation, regarding the treatment with Au (III) and Au (I) was found, it may be assumed that slightly higher cytotoxicity on fibroblasts was displayed than on macrophages when Au (III) was compared to Au (I). As conclusion, Au (III) and Au (I) bactericidal concentrations were not as devastating in mammalian cells as they were in *E. coli* cultures corroborating our previous studies [12,21].

4. Conclusions

The antimicrobial action of gold species, specifically Au (III) and Au (I), has been successfully elucidated in our work. We have

observed differential effects after treatment of Gram-positive and Gram-negative bacteria with Au (III) and Au (I) species, being significantly more efficient in decreasing *E. coli* viability at the concentrations tested (31.25–250 μM). The novelty of our work is the combined molecular mechanistic study on the toxicity of Au species by the analysis of five different mechanisms of antimicrobial action. Further studies regarding electronic microscopy and FTIR highlighted the superior antimicrobial action of Au (III) vs Au (I) in terms of cell wall damage, ROS production, and intracellular components leakage. In-depth *E. coli* genomic and proteomic studies displayed different mechanisms of action for Au (III) and Au (I) species regarding oxidative stress, bacterial energetic metabolism, biosynthetic processes, and cell transport, thus further confirming the superior toxicity of Au (III) vs Au (I) species. Moreover, on eukaryotic cells the ionic gold species analyzed did not show significant harmful effects at the doses tested, although ROS generation and mitochondrial membrane potential perturbations were identified after gold treatment. However, these effects did not exert critical consequences on cell viability nor morphology. The results of our research emphasize the relevance of the search for novel efficient bactericidal compounds and the important role of gold in bacterial cytotoxicity without damaging mammalian cells.

CRediT authorship contribution statement

Monica Paesa: Methodology, Software, Validation, Formal analysis, Data curation, Writing – original draft, Visualization. **Cristina Remirez de Ganuza:** Methodology, Formal analysis, Data curation, Writing – original draft, Visualization. **Teresa Alejo:** Methodology, Formal analysis, Writing – review & editing. **Cristina Yus:** Methodology, Formal analysis, Writing – review & editing. **Silvia Irusta:** Methodology, Investigation, Writing – review & editing, Supervision. **Manuel Arruebo:** Conceptualization, Resources, Investigation, Writing – original draft, Writing – review & editing, Supervision, Visualization, Project administration, Funding acquisition. **Víctor Sebastian:** Conceptualization, Methodology, Formal analysis, Investigation, Resources, Writing – review & editing, Supervision. **Gracia Mendoza:** Conceptualization, Methodology, Validation, Resources, Investigation, Writing – review & editing, Supervision, Visualization, Project administration, Funding acquisition.

Data availability

Data will be made available on request.

Declaration of Competing Interest

The authors declare that they have no known competing financial interests or personal relationships that could have appeared to influence the work reported in this paper.

Acknowledgements

Financial support from the Spanish Ministry of Science and Innovation (grant numbers PID2020-113987RB-I00, PID2021-127847OB-I00 and CTQ2017-84473-R) is gratefully acknowledged. CIBER-BBN is an initiative funded by the VI National R&D&i Plan 2008-2011 financed by the Instituto de Salud Carlos III with the assistance of the European Regional Development Fund. We acknowledge the ELECMI-LMA-INA (University of Zaragoza, Spain), Nanbiosis ICTS, the Genomics Core Unit from Instituto de Investigaciones Biomédicas Alberto Sols (Madrid, Spain), and Cell Culture, Cell Separation and Flow Cytometry, Genomics and Proteomics Core Units from IACS/IIS Aragon for facilitating the access to their instruments and expertise. We would like to thank Dr. Gema Rodríguez-Tarduchy for helpful advice regarding genomics studies. M.P. and C.R. acknowledge the support from Aragon regional government (Orden CUS/581/2020 and Orden CUS/803/2021, respectively). G.M. gratefully acknowledges the support from the Miguel Servet Program (MS19/00092; Instituto de Salud Carlos III).

Appendix A. Supplementary data

Supplementary data to this article can be found online at https://doi.org/10.1016/j.jcis.2022.11.138.

References

[1] U.. D. of H. and H. Services, Antibiotic resistance threats in the United States, Centers Dis. Control Prev. (2019) 1–113. https://www.cdc.gov/drugresistance/biggest_threats.html.
[2] A. Cassini, L.D. Högberg, D. Plachouras, A. Quattrocchi, A. Hoxha, G.S. Simonsen, M. Colomb-Cotinat, M.E. Kretzschmar, B. Devleesschauwer, M. Cecchini, D.A. Ouakrim, T.C. Oliveira, M.J. Struelens, C. Suetens, D.L. Monnet, R. Strauss, K. Mertens, T. Struyf, B. Catry, K. Latour, I.N. Ivanov, E.G. Dobreva, A. Tambic Andraševic, S. Soprek, A. Budimir, N. Paphitou, H. Žemlicková, S. Schytte Olsen, U. Wolff Sönksen, P. Märtin, M. Ivanova, O. Lyytikäinen, J. Jalava, B. Coignard, T. Eckmanns, M. Abu Sin, S. Haller, G.L. Daikos, A. Gikas, S. Tsiodras, F. Kontopidou, Á. Tóth, Á. Hajdu, Ó. Guólaugsson, K.G. Kristinsson, S. Murchan, K. Burns, P. Pezzotti, C. Gagliotti, U. Dumpis, A. Liuimiene, M. Perrin, M.A. Borg, S.C. de Greeff, J.C. Monen, M.B. Koek, P. Elstrøm, D. Zabicka, A. Deptula, W. Hryniewicz, M. Caniça, P.J. Nogueira, P.A. Fernandes, V. Manageiro, G.A. Popescu, R.I. Serban, E. Schréterová, S. Litvová, M. Štefkovicová, J. Kolman, I. Klavs, A. Korošec, B. Aracil, A. Asensio, M. Pérez-Vázquez, H. Billström, S. Larsson, J.S. Reilly, A. Johnson, S. Hopkins, Attributable deaths and disability-adjusted life-years caused by infections with antibiotic-resistant bacteria in the EU and the European Economic Area in 2015: a population-level modelling analysis, Lancet Infect. Dis. 19 (2019) 56–66. https://doi.org/10.1016/S1473-3099(18)30605-4.
[3] J.A. Lemire, J.J. Harrison, R.J. Turner, Antimicrobial activity of metals: Mechanisms, molecular targets and applications, Nat. Rev. Microbiol. 11 (2013) 371–384, https://doi.org/10.1038/nrmicro3028.
[4] G. Zhao, S.E. Stevens, Multiple parameters for the comprehensive evaluation of the susceptibility of Escherichia coli to the silver ion, BioMetals 11 (1998) 27–32, https://doi.org/10.1023/A:1009253223055.
[5] H.J. Johnston, G. Hutchison, F.M. Christensen, S. Peters, S. Hankin, V. Stone, A review of the in vivo and in vitro toxicity of silver and gold particulates: Particle attributes and biological mechanisms responsible for the observed toxicity, Crit. Rev. Toxicol. 40 (2010) 328–346, https://doi.org/10.3109/10408440903453074.
[6] L. Guo, I. Panderi, D.D. Yan, K. Szulak, Y. Li, Y.T. Chen, H. Ma, D.B. Niesen, N. Seeram, A. Ahmed, B. Yan, D. Pantazatos, W. Lu, A comparative study of hollow copper sulfide nanoparticles and hollow gold nanospheres on degradability and toxicity, ACS Nano 7 (2013) 8780–8793, https://doi.org/10.1021/nn403202w.
[7] L. Yang, H. Kuang, W. Zhang, Z.P. Aguilar, H. Wei, H. Xu, Comparisons of the biodistribution and toxicological examinations after repeated intravenous administration of silver and gold nanoparticles in mice, Sci. Rep. 7 (2017) 1–12, https://doi.org/10.1038/s41598-017-03015-1.
[8] A. Balfourier, N. Luciani, G. Wang, G. Lelong, O. Ersen, A. Khelfa, D. Alloyeau, F. Gazeau, F. Carn, Unexpected intracellular biodegradation and recrystallization of gold nanoparticles, Proc. Natl. Acad. Sci. U. S. A. 117 (2020) 103–113, https://doi.org/10.1073/PNAS.1911734116/-/DCSUPPLEMENTAL.
[9] Y. Zhang, T.P. Shareena Dasari, H. Deng, H. Yu, Antimicrobial Activity of Gold Nanoparticles and Ionic Gold, J. Environ. Sci. Heal. - Part C, Environ. Carcinog. Ecotoxicol. Rev. 33 (2015) 286–327, https://doi.org/10.1080/10590501.2015.1055161.
[10] C. Muñoz-Villagrán, F. Contreras, F. Cornejo, M. Figueroa, D. Valenzuela-Bezanilla, R. Luraschi, C. Reinoso, J. Rivas-Pardo, J. Rivas-Pardo, C. Vásquez, M. Castro, F. Arenas, Understanding gold toxicity in aerobically-grown Escherichia coli, Biol. Res. 53 (2020) 1–9, https://doi.org/10.1186/s40659-020-00292-5.
[11] F.U. Khan, Y. Chen, N.U. Khan, A. Ahmad, K. Tahir, Z.U.H. Khan, A.U. Khan, S.U. Khan, M. Raza, P. Wan, Visible light inactivation of E. coli, Cytotoxicity and ROS determination of biochemically capped gold nanoparticles, Microb. Pathog. 107 (2017) 419–424, https://doi.org/10.1016/j.micpath.2017.04.024.
[12] A. Regiel-Futyra, M. Kus-Liśkiewicz, V. Sebastian, S. Irusta, M. Arruebo, G. Stochel, A. Kyzioł, Development of noncytotoxic chitosan-gold nanocomposites as efficient antibacterial materials, ACS Appl. Mater. Interfaces 7 (2) (2015) 1087–1099, https://doi.org/10.1021/am508094e.
[13] Y. Cui, Y. Zhao, Y. Tian, W. Zhang, X. Lü, X. Jiang, The molecular mechanism of action of bactericidal gold nanoparticles on Escherichia coli, Biomaterials 33 (2012) 2327–2333, https://doi.org/10.1016/j.biomaterials.2011.11.057.
[14] W. Vollmer, D. Blanot, M.A. De Pedro, Peptidoglycan structure and architecture, FEMS Microbiol. Rev. 32 (2008) 149–167, https://doi.org/10.1111/j.1574-6976.2007.00094.x.

[15] H.W. Wang, Y. Chen, H. Yang, X. Chen, M.X. Duan, P.C. Tai, S.F. Sui, Ring-like pore structures of SecA: Implication for bacterial protein-conducting channels, Proc. Natl. Acad. Sci. U.S.A. 100 (2003) 4221–4226, https://doi.org/10.1073/pnas.0737415100.
[16] K. Zheng, M.I. Setyawati, D.T. Leong, J. Xie, Overcoming bacterial physical defenses with molecule-like ultrasmall antimicrobial gold nanoclusters, Bioact. Mater. 6 (2021) 941–950, https://doi.org/10.1016/j.bioactmat.2020.09.026.
[17] F. Reith, B. Etschmann, C. Grosse, H. Moors, M.A. Benotmane, P. Monsieurs, G. Grass, C. Doonan, S. Vogt, B. Lai, G. Martinez-Criado, G.N. George, D.H. Nies, M. Mergeay, A. Pring, G. Southam, J. Brugger, Mechanisms of gold biomineralization in the bacterium Cupriavidus metallidurans, Proc. Natl. Acad. Sci. U.S.A. 106 (2009) 17757–17762, https://doi.org/10.1073/pnas.0904583106.
[18] F. Kang, X. Qu, P.J.J. Alvarez, D. Zhu, Extracellular Saccharide-Mediated Reduction of Au3+ to Gold Nanoparticles: New Insights for Heavy Metals Biomineralization on Microbial Surfaces, Environ. Sci. Technol. 51 (2017) 2776–2785, https://doi.org/10.1021/acs.est.6b05930.
[19] T.S. Dasari, Y. Zhang, H. Yu, Antibacterial Activity and Cytotoxicity of Gold (I) and (III) Ions and Gold Nanoparticles, Biochem. Pharmacol. Open Access. 4 (2015), https://doi.org/10.4172/2167-0501.1000199.
[20] M.R. Torres, A.J. Slate, S.F. Ryder, M. Akram, C.J.C. Iruzubieta, K.A. Whitehead, Ionic gold demonstrates antimicrobial activity against Pseudomonas aeruginosa strains due to cellular ultrastructure damage, Arch. Microbiol. 203 (2021) 3015–3024, https://doi.org/10.1007/S00203-021-02270-1.
[21] G. Mendoza, A. Regiel-Futyra, V. Andreu, V. Sebastián, A. Kyzioł, G. Stochel, M. Arruebo, Bactericidal Effect of Gold-Chitosan Nanocomposites in Coculture Models of Pathogenic Bacteria and Human Macrophages, ACS Appl. Mater. Interfaces. 9 (2017) 17693–17701, https://doi.org/10.1021/ACSAMI.6B15123.
[22] S. Dasari TP, Z. Y, Antibacterial Activity and Cytotoxicity of Gold (I) and (III) Ions and Gold Nanoparticles, Biochem. Pharmacol. Open Access. 04 (06) (2015), https://doi.org/10.4172/2167-0501.1000199.
[23] X. Gu, Z. Xu, L. Gu, H. Xu, F. Han, B. Chen, X. Pan, Preparation and antibacterial properties of gold nanoparticles: a review, Environ. Chem. Lett. 19 (2021) 167–187, https://doi.org/10.1007/s10311-020-01071-0.
[24] A.H. Delcour, A.H. Delcour, NIH Public Access 1794 (5) (2010) 808–816, https://doi.org/10.1016/j.bbapap.2008.11.005.Outer.
[25] R.C. Fahey, W.C. Brown, W.B. Adams, M.B. Worsham, Occurrence of glutathione in bacteria, J. Bacteriol. 133 (1978) 1126–1129, https://doi.org/10.1128/jb.133.3.1126-1129.1978.
[26] Shareena Dashari TP, Zhang Y, Yu H, Antibacterial Activity and Cytotoxicity of Gold (I) and (III) Ions and Gold Nanoparticles, Biochem Pharmacol (Los Angel) 199 (2015), https://doi.org/10.4172/2167-0501.1000199.
[27] X. Jiang, C. Zhao, X. Fan, G. Wu, Gold Biomineralization on Bacterial Biofilms for Leaching of Au3+ Damages Eukaryotic Cells, ACS Omega 4 (2019) 16667–16673, https://doi.org/10.1021/acsomega.9b02601.
[28] Q. Wang, F. Kang, Y. Gao, X. Mao, X. Hu, Sequestration of nanoparticles by an EPS matrix reduces the particle-specific bactericidal activity, Sci. Rep. 6 (2016) 1–10, https://doi.org/10.1038/srep21379.
[29] F. Faghihzadeh, N.M. Anaya, C. Astudillo-Castro, V. Oyanedel-Craver, Kinetic, metabolic and macromolecular response of bacteria to chronic nanoparticle exposure in continuous culture, Environ. Sci. Nano 5 (2018) 1386–1396, https://doi.org/10.1039/c8en00325d.
[30] F. Faghihzadeh, N.M. Anaya, L.A. Schifman, V. Oyanedel-Craver, Fourier transform infrared spectroscopy to assess molecular-level changes in microorganisms exposed to nanoparticles, Nanotechnol. Environ. Eng. 1 (2016) 1–16, https://doi.org/10.1007/s41204-016-0001-8.
[31] M. Mathelié-Guinlet, A.T. Asmar, J.F. Collet, Y.F. Dufrêne, Lipoprotein Lpp regulates the mechanical properties of the E. coli cell envelope, Nat. Commun. 11 (2020), https://doi.org/10.1038/s41467-020-15489-1.
[32] N. Dave, A. Troullier, I. Mus-Veteau, M. Duñach, G. Leblanc, E. Padrós, Secondary structure components and properties of the melibiose permease from Escherichia coli: A fourier transform infrared spectroscopy analysis, Biophys. J. 79 (2000) 747–755, https://doi.org/10.1016/S0006-3495(00)76332-6.
[33] B. Ramalingam, T. Parandhaman, S.K. Das, Antibacterial Effects of Biosynthesized Silver Nanoparticles on Surface Ultrastructure and Nanomechanical Properties of Gram-Negative Bacteria viz. Escherichia coli and Pseudomonas aeruginosa, ACS Appl. Mater. Interfaces 8 (2016) 4963–4976, https://doi.org/10.1021/acsami.6b00161.
[34] Q. Abu-Salem, M.K. Harb, C. Maichle-Mößmer, M. Steimann, W. Voelter, Synthesis and structural characterization of a gold(I) complex containing 1,3-dimethylcyanurate ligand, Arab. J. Chem. 10 (2017) S3883–S3888, https://doi.org/10.1016/j.arabjc.2014.05.027.
[35] Z. Filip, S. Hermann, K. Demnerová, FT-IR spectroscopic characteristics of differently cultivated Escherichia coli, Czech J. Food Sci. 26 (2008) 458–463, https://doi.org/10.17221/14/2008-cjfs.
[36] C. Saulou-Bérion, I. Gonzalez, B. Enjalbert, J.-N. Audinot, I. Fourquaux, F. Jamme, M. Cocaign-Bousquet, M. Mercier-Bonin, L. Girbal, Y.-J. Wang, Escherichia coli under ionic silver stress: An integrative approach to explore transcriptional, physiological and biochemical responses, PLoS One 10 (12) (2015) e0145748, https://doi.org/10.1371/journal.pone.0145748.
[37] T. Cetinkaya, W. Wijaya, F. Altay, Z. Ceylan, Fabrication and characterization of zein nanofibers integrated with gold nanospheres, LWT 155 (2022), https://doi.org/10.1016/J.LWT.2021.112976 112976.
[38] V.D. Badwaik, L.M. Vangala, D.S. Pender, C.B. Willis, Z.P. Aguilar, M.S. Gonzalez, R. Paripelly, R. Dakshinamurthy, Size-dependent antimicrobial properties of sugarencapsulated gold nanoparticles synthesized by a green method, Nanoscale Res. Lett. 7 (2012) 1–11, https://doi.org/10.1186/1556-276X-7-623/FIGURES/7.
[39] M.D. Urović, R. Puchta, Ž.D. Bugarčić, R. Van Eldik, Studies on the reactions of [AuCl4]- with different nucleophiles in aqueous solution, Dalt. Trans. 43 (2014) 8620–8632, https://doi.org/10.1039/c4dt00247d.
[40] N.G. Khlebtsov, Determination of size and concentration of gold nanoparticles from extinction spectra, Anal. Chem. 80 (2008) 6620–6625, https://doi.org/10.1021/ac800834n.
[41] X. Huang, M.A. El-Sayed, Gold nanoparticles: Optical properties and implementations in cancer diagnosis and photothermal therapy, J. Adv. Res. 1 (2010) 13–28, https://doi.org/10.1016/j.jare.2010.02.002.
[42] C. Garin, T. Alejo, V. Perez-Laguna, M. Prieto, G. Mendoza, M. Arruebo, V. Sebastian, A. Rezusta, Chalcogenide nanoparticles and organic photosensitizers for synergetic antimicrobial photodynamic therapy, J. Mater. Chem. B. 9 (2021) 6246–6259, https://doi.org/10.1039/d1tb00972a.
[43] M. Arsenijevic, M. Milovanovic, V. Volarevic, A. Djekovic, T. Kanjevac, N. Arsenijevic, S. Dukic, Z.D. Bugarcic, Cytotoxicity of gold(III) Complexes on A549 Human Lung Carcinoma Epithelial Cell Line, Med. Chem. (Los. Angeles). 8 (2012) 2–8, https://doi.org/10.2174/157340612799278469.
[44] A. Habib, T. Hara, A. Nargis, E. Nyarko, M. Tabata, DNA cleavage and trypanosomes death by a combination of Alamar blue and Au(III), J. Chem. Soc. Pakistan 42 (2020) 141–148, https://doi.org/10.52568/000614.
[45] R. Hengge-Aronis, Signal Transduction and Regulatory Mechanisms Involved in Control of the σ S (RpoS) Subunit of RNA Polymerase, Microbiol. Mol. Biol. Rev. 66 (2002) 373–395, https://doi.org/10.1128/mmbr.66.3.373-395.2002.
[46] W.A. Prinz, F. Åslund, A. Holmgren, J. Beckwith, The role of the thioredoxin and glutaredoxin pathways in reducing protein disulfide bonds in the Escherichia coli cytoplasm, J. Biol. Chem. 272 (1997) 15661–15667, https://doi.org/10.1074/jbc.272.25.15661.
[47] C. Michán, M. Manchado, G. Dorado, C. Pueyo, In vivo transcription of the Escherichia coli oxyR regulon as a function of growth phase and in response to oxidative stress, J. Bacteriol. 181 (1999) 2759–2764, https://doi.org/10.1128/jb.181.9.2759-2764.1999.
[48] A.K. Holm, L.M. Blank, M. Oldiges, A. Schmid, C. Solem, P.R. Jensen, G.N. Vemuri, Metabolic and Transcriptional Response to Cofactor Perturbations in Escherichia coli, J. Biol. Chem. 285 (2010) 17498–17506, https://doi.org/10.1074/JBC.M109.095570.
[49] Q. Zhong, B. Kobe, U. Kappler, Molybdenum Enzymes and How They Support Virulence in Pathogenic Bacteria, Front. Microbiol. 11 (2020) 3185, https://doi.org/10.3389/FMICB.2020.615860/BIBTEX.
[50] M. Marcén, G. Cebrián, V. Ruiz-Artiga, S. Condón, P. Mañas, Protective effect of glutathione on Escherichia coli cells upon lethal heat stress, Food Res. Int. 121 (2019) 806–811, https://doi.org/10.1016/j.foodres.2018.12.063.
[51] T. Friedrich, The NADH:ubiquinone oxidoreductase (complex I) from Escherichia coli, Biochim. Biophys. Acta. 1364 (1998) 134–146, https://doi.org/10.1016/S0005-2728(98)00024-3.
[52] G. Deckers-Hebestreit, J.C. Greie, W.D. Stalz, K. Altendorf, The ATP synthase of Escherichia coli: structure and function of F0 subunits, Biochim. Biophys. Acta - Bioenerg. 1458 (2000) 364–373, https://doi.org/10.1016/S0005-2728(00)00087-6.
[53] U. Choi, C.R. Lee, Distinct Roles of Outer Membrane Porins in Antibiotic Resistance and Membrane Integrity in Escherichia coli, Front. Microbiol. 10 (2019) 953, https://doi.org/10.3389/FMICB.2019.00953/BIBTEX.
[54] R. Choudhury, S. Srivastava, Zinc resistance mechanisms in bacteria, Curr. Sci. 81 (2001) 768–775.
[55] S. Franke, G. Grass, C. Rensing, D.H. Nies, Molecular Analysis of the Copper-Transporting Efflux System CusCFBA of Escherichia coli, J. Bacteriol. 185 (13) (2003) 3804–3812, https://doi.org/10.1128/JB.185.13.3804-3812.2003.
[56] ISO 10993-5:2009 Biological evaluation of medical devices — Part 5: Tests for in vitro cytotoxicity, (n.d.). https://www.iso.org/standard/36406.html (accessed June 17, 2022).
[57] H. Sivaram, J. Tan, H.V. Huynh, Syntheses, characterizations, and a preliminary comparative cytotoxicity study of gold(I) and gold(III) complexes bearing benzimidazole- and pyrazole-derived N-heterocyclic carbenes, Organometallics 31 (2012) 5875–5883, https://doi.org/10.1021/om300444c.
[58] H. Ragab Khalil Ali, M. Ms, In Vitro Study for Comparing the Cytotoxicity of Silver and Gold Nanospheres on Raw 264.7 Murine Macrophage Cell Line, J. Bacteriol. Parasitol. 07 (02) (2016), https://doi.org/10.4172/2155-9597.1000264.
[59] Q. Zhang, V.M. Hitchins, A.M. Schrand, S.M. Hussain, P.L. Goering, Uptake of gold nanoparticles in murine macrophage cells without cytotoxicity or production of pro-inflammatory mediators, Nanotoxicology 5 (2011) 284–295, https://doi.org/10.3109/17435390.2010.512401.
[60] B. Pem, I.M. Pongrac, L. Ulm, I. Pavičić, V. Vrček, D.D. Jurašin, M. Ljubojević, A. Krivohlavek, I.V. Vrček, Toxicity and safety study of silver and gold nanoparticles functionalized with cysteine and glutathione, Beilstein J. Nanotechnol. 10 (2019) 1802–1817, https://doi.org/10.3762/bjnano.10.175.
[61] S.L. Best, P.J. Sadler, Gold drugs: Mechanism of action and toxicity, Gold Bull 29 (1996) 87–93, https://doi.org/10.1007/BF03214741.
[62] D. Drescher, H. Traub, T. Büchner, N. Jakubowski, J. Kneipp, Properties of in situ generated gold nanoparticles in the cellular context, Nanoscale 9 (2017) 11647–11656, https://doi.org/10.1039/c7nr04620k.